Experimental and theoretical simulations of climbing falls

Martyn Pavier

Department of Mechanical Engineering, University of Bristol, Bristol, BS8 1TR

Abstract

A modern rock climber attempting difficult routes will expect to take a number of falls. Typically the falls will be from the same point on the climb, for example at a particularly difficult series of moves, therefore the same part of the climbing rope will be damaged by each fall. Since the consequences of rope failure are serious, it is important that the climber should be aware of the number of falls the rope can withstand.

The work described in this paper was carried out to understand the mechanics of climbing falls so as to enable predictions to be made of the tension developed in the rope. Once the value for this tension is known, an estimation can be made of the life of the rope measured as the number of falls to failure.

A theoretical simulation of climbing falls has been developed which includes the nonlinearity of the rope behaviour and friction where the rope runs through 'karabiners,' the metal clips used to anchor the climbers to the rock. The results of the simulation have been compared to experimentally measured rope tensions.

The number of falls to failure has been measured experimentally for various lengths of fall and fall factors (the ratio of the length of fall to the length of rope). Failure of the rope invariably occurs where the rope runs over the most heavily loaded karabiner; therefore, the karabiner edge radius has also been varied. The experimental data have been used to derive a failure curve for the rope that may be combined with the theoretical simulation to predict the number of falls to failure.

Keywords: Climbing; failure analysis; mechanics; theoretical simulation.

Notation

d	Vertical distance above last runner
g	Acceleration due to gravity
k	Modulus of rope for linear elastic model
k_1, k_2	Moduli of rope for visco-elastic model
l_i	Length of rope segment i
n	Number of rope segments
r	Runner radius
s_i	Total slip at runner i
x_i, y_i	Co-ordinates of runner i
$\mathbf{C}$	Matrix relating incremental slips to incremental strains

Correspondence Address:
Martyn Pavier, Department of Mechanical Engineering,
University of Bristol, Bristol BS8 1TR, U.K.
E-mail: martyn.pavier@bristol.ac.uk

$\dot{E}$ Rate of energy dissipation at a runner due to friction
F Fall factor
$\mathbf{I}$ Unit matrix
$\mathbf{K}$ Matrix relating incremental strains to incremental tensions
L Length of rope run-out
$\mathbf{L}$ Matrix of slip conditions
M Mass of leader
S Critical tension in rope segment 1 for slip at belay
T_i Total tension in rope segment i
$\mathbf{T}$ Vector of total tensions
ε_i Total strain in rope segment i
η_i Maximum tension ratio at runner i
λ Viscous coefficient of rope for visco-elastic model
μ_i Coefficient of friction at runner i
θ_i Angle of lap at runner i
σ_i Slip condition at runner i
Δs_i Incremental slip at runner i
$\Delta\mathbf{s}$ Vector of incremental slips
Δt Duration of the increment of time
ΔT_i Incremental tension in rope segment i
$\Delta\mathbf{T}$ Vector of incremental tensions
$\Delta\varepsilon_i$ Incremental strain in rope segment i
$\boldsymbol{\Delta\varepsilon}$ Vector of incremental strains

Introduction

The modern rock climber puts considerable trust in the rope: falls while climbing are commonplace, particularly for experienced climbers attempting difficult routes, and the consequences of rope failure are usually very serious. Consequently, climbing ropes are of a sophisticated construction, combining low mass with high strength and energy absorbing properties. The modern climbing rope is of a kernmantle type construction as shown in Fig. 1, consisting of a twisted nylon kern (the load-

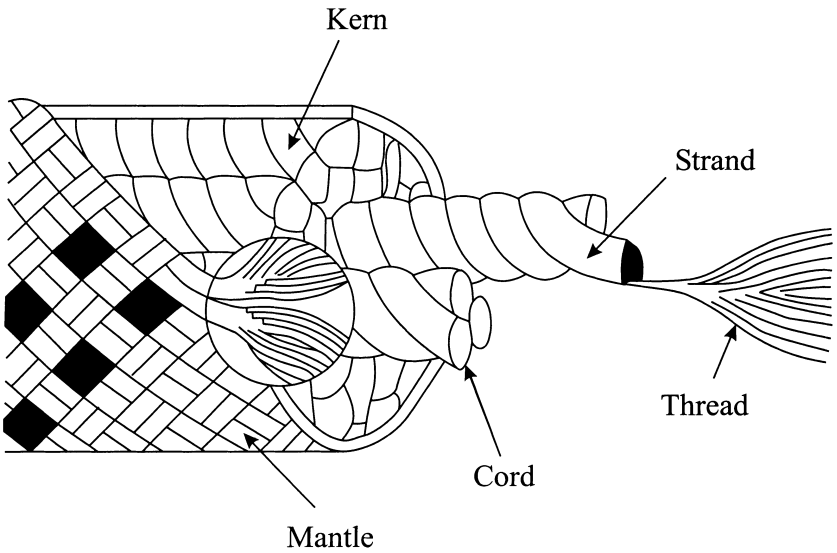

Figure 1 Construction of a kernmantle climbing rope.

bearing part of the rope) and a woven nylon mantle to protect the kern from abrasion. The kern is made up from a number of cords, the cords in turn being made from several strands twisted together. Each strand is itself formed from nylon threads, each of about 25 μm diameter. A typical rope has approximately five million threads. The rope is designed to decelerate a falling climber without subjecting the body to very high forces.

Climbers should understand the effect on their rope of any climbing falls so that they are able to decide whether the strength of the rope has been reduced sufficiently for it to be retired from service. Currently, climbers rely on rule-of-thumb methods to assess the effects of falls on their ropes, but the understanding of the physical processes involved during falls is often poor. Fortunately, climbing rope failures are not common, and when they do occur are usually because of other factors, for example the rope running over the sharp edge of a rock. Nevertheless, studies have shown (Microys 1983) that even experienced climbers may have little appreciation of the current state of their ropes, and in some cases their ropes may be close to the end of their useful lives.

The research described in this paper aims to provide a more precise description of a climbing fall and therefore give a better appreciation of the tension developed in the rope. Such an appreciation may be combined with a model for the degradation of the rope so as to provide a procedure for the life prediction assessment of a climbing rope.

Little previous work of this nature exists; however, Schubert (1986) provides some data on tensions developed in climbing ropes and a description of what influences these tensions, although the work is largely descriptive. In addition, there have been some previous reports of experimental measurements of tensions developed in climbing ropes during falls (see for example Perkins 1987).

In this paper, the procedures involved in climbing and the circumstances leading to a fall are first described. A simple analysis of a climbing fall is provided as an introduction to the subsequent theoretical analysis. The theoretical analysis is then presented with predictions of the tensions developed in the rope which are compared with experimental tests. Finally, a series of experimental tests are carried out to derive a failure curve for the rope that can be used to predict the number of falls to failure for a particular fall situation.

Background to rock climbing

Smith (1996) presented an interesting account of the development of the procedures involved in rock climbing. Usually climbers climb as a pair: for example, a female leading climber (or leader) and a second male climber (or second). The second belays himself to the rock face, by attaching himself, via his harness, to anchors fixed to the rock. These anchors take various forms, but typically they may be nuts (metal wedges) jammed into cracks, pitons (metal spikes) hammered into cracks or slings of rope draped over a rock spike. The leader climbs above the second to the top of the rock face, or until she can find a safe place to belay herself. Once the leader is belayed, the second removes his belay and climbs to rejoin the leader. As the second climbs, the leader takes in the rope so as to protect the second should he slip.

The critical part of the climbing procedure is as the leader climbs above her second. To make this stage safer, the leader will run the rope through karabiners (metal clips) attached to additional anchors fixed to the rock. These additional anchors are known as running belays (or runners). A situation during a climb where the leader has fixed three running belays may then be as shown in Fig. 2. Should the leader fall from the rock, the distance she falls until the rope begins to decelerate her will be twice the distance from the last running belay, assuming this was vertically beneath her. As the leader climbs, the second pays the rope out through a belay device attached to his harness. The belay device is designed to make it easy for the second to hold the rope tight in the event of a fall. The rope from second to leader is referred to as the live rope. The remaining part of the rope yet to be paid out by the second is known as the dead rope.

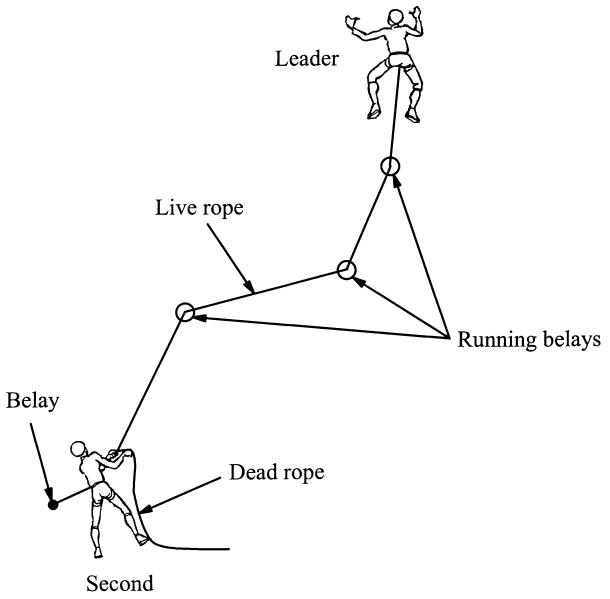

Figure 2 Description of terms used in climbing.

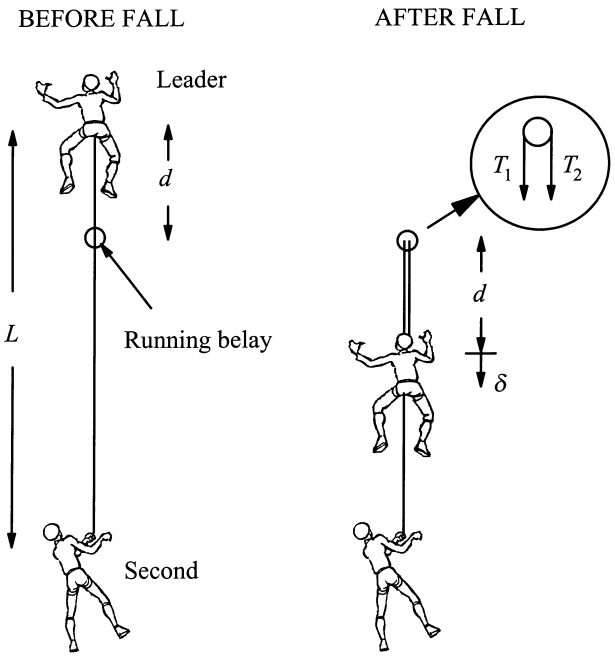

Figure 3 Geometry of a simple climbing fall.

Experienced climbers undertaking a difficult climb may expect to take a number of falls during the climb. These falls inevitably lead to a deterioration in the rope and it is therefore useful for the climber to have an appreciation of the factors controlling the magnitude of the tensions developed in the rope. The traditional measure of the severity of a fall has been the fall factor, the ratio of the length of the fall to the length of rope between the leader and the second. The fall factor varies from zero when the leader falls just after placing a runner, to two when the leader falls before she has been able to place any runners. This fall factor approach implicitly assumes the rope behaves in a linear elastic manner and takes no account of the slip through the belay device and friction of the rope over the runners.

Later in this paper, a theoretical procedure will be developed for taking into account these effects. First an analytical expression for the maximum tension in the rope will be found using the standard fall factor approach (Wexler 1950) to demonstrate the basic mechanics of climbing falls.

Figure 3 shows a simple climbing fall where the leader of mass M, falls from a distance d above her last runner. The fall factor F is given by

$$F = \frac{2d}{L} \tag{1}$$

where L is the length of live rope. The leader falls a distance $2d$ before the rope begins to tighten plus a further distance δ before coming to a halt due to stretch in the rope. The loss of potential energy of the leader due to the loss of height is $Mg(2d + \delta)$. This potential energy is transferred into strain energy stored in the rope of $k\delta^2/(2L)$. Here, g is the acceleration due to gravity and k is the elastic modulus of the rope. From the principle of conservation of energy the further distance δ is calculated to be

$$\delta = \frac{M\,gL}{k}\left[1 + \sqrt{1 + \frac{2kF}{Mg}}\right]$$

and hence the maximum tension in the rope is found to be

$$T = Mg\left[1 + \sqrt{1 + \frac{2kF}{Mg}}\right] \tag{2}$$

This analysis leads to the conclusion that the maximum tension in the rope is controlled by the

fall factor, the mass of the climber and the stiffness of the rope, but not by the absolute length of the fall.

When the modulus of elasticity of the rope can be assumed to be much larger than the weight of the falling climber, a simplified calculation for the maximum tension may be written as:

$$T = \sqrt{2kFMg} \tag{3}$$

Theoretical analysis of climbing falls

A theoretical analysis of climbing falls is now presented which includes slip at the belay, friction at runners and a more realistic model for the behaviour of the rope. The analysis uses an incremental approach, necessitating the use of a computer, but allowing the analysis of a fall situation with an arbitrary number of runners. The results give tensions in individual rope segments, loads at runners, slip through the belay device and the position of the falling climber.

First, the geometry of a pitch is described using a two-dimensional Cartesian co-ordinate system with the second at the origin (Fig. 4). The leader has placed $n - 1$ runners, dividing the rope into n segments. Runner i is located at x_i, y_i. The leader falls from a point, distance d, vertically above her last runner. Calculation provides the original length l_i of rope segment i between runners $i - 1$ and i, the angle of lap θ_i at runner i and the total length of rope run out L. A maximum tension ratio η_i is calculated for each runner from

$$\eta_i = e^{\mu_i \theta_i} \tag{4}$$

where μ_i is the coefficient of friction at runner i. The tension ratio relates the tensions for rope segments on each side of a runner when the rope slips over the runner. Experimental measurements of the tension in the rope segments on each side of

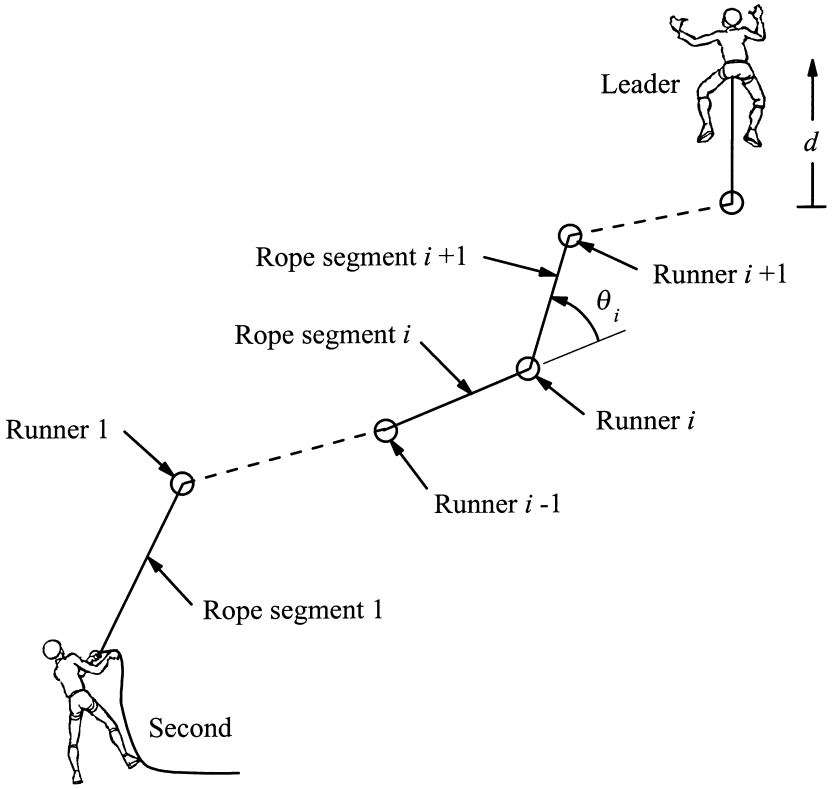

Figure 4 Description of pitch geometry used in the theoretical simulation.

the runner have been made for different angles of lap. These measurements confirm the exponential form of eqn (4) and show a coefficient of friction of 0.18–0.22 between steel and rope.

The relationship between the strain in each rope segment and the total slip at each runner is now considered. Taking segment i (Fig. 5):

$$s_i(1+\varepsilon_i) - s_{i-1}(1+\varepsilon_i) = \varepsilon_i l_i \tag{5}$$

where ε_i is the strain in rope segment i and s_i is the total slip at runner i, the slip being positive in the direction from the second to the leader and measured with zero strain in the rope. An incremental form of eqn (5) may be derived:

$$\Delta s_i(1+\varepsilon_i) - \Delta s_{i-1}(1+\varepsilon_i) = \Delta\varepsilon_i(l_i + s_{i-1} - s_i) \tag{6}$$

where $\Delta\varepsilon_i$ is the incremental strain in rope segment i and Δs_i the incremental slip at runner i. Eqns (5) and (6) are also valid for the first rope segment if s_0 and Δs_0 are taken to be the slip and incremental slip through the belay device. The final rope segment, between the leader and her last runner, gives a modified version of eqns (5) and (6):

$$s_n - s_{n-1}(1+\varepsilon_n) = \varepsilon_n d \tag{7}$$

$$\Delta s_n - \Delta s_{n-1}(1+\varepsilon_n) = \Delta\varepsilon_n(d + s_{n-1}) \tag{8}$$

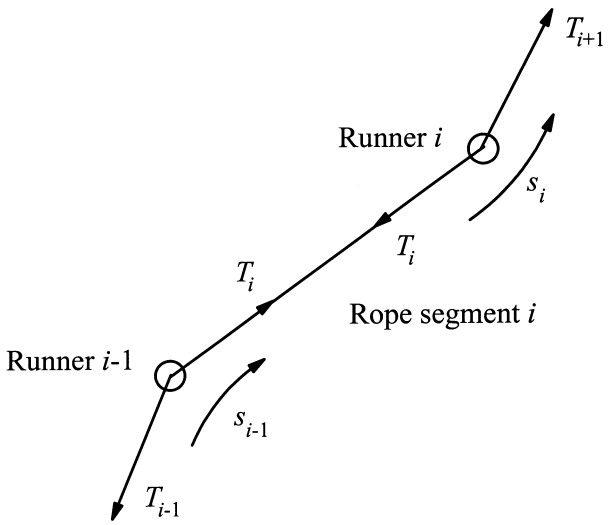

Figure 5 Notation used for tensions and slips in an individual rope segment.

where s_n and Δs_n are the position and incremental position of the leader measured positive downwards relative to the point at which the rope becomes tight. That is, the origin for s_n is a distance d vertically below the last runner. For small increments, Δs_n is given by

$$\Delta s_n = \dot{s}_n \Delta t \tag{9}$$

where $\dot{s}_n$ is the velocity of the leader and Δt the duration of the increment of time.

A matrix equation can now be formulated giving the vector of incremental strains in each rope segment $\boldsymbol{\Delta\varepsilon}$ in terms of the vector of incremental slips $\boldsymbol{\Delta s}$

$$\mathbf{C}\boldsymbol{\Delta s} = \boldsymbol{\Delta\varepsilon} \tag{10}$$

where $\boldsymbol{\Delta s}^T = [\Delta s_0 \ldots \Delta s_i \ldots \Delta s_n]$ and $\boldsymbol{\Delta\varepsilon}^T = [\Delta\varepsilon_0 \ldots \Delta\varepsilon_i \ldots \Delta\varepsilon_n]$ Note that matrix $\mathbf{C}$ has dimension n by $n+1$. A typical row of matrix $\mathbf{C}$ relating the incremental strain in rope segment 4 to the incremental slips at runners 3 and 4 has the form:

$$\begin{bmatrix} & & 0 & 0 & & \\ & & \vdots & \vdots & & \\ 0 & \cdots & \frac{-1-\varepsilon_4}{l_4+s_3-s_4} & \frac{1+\varepsilon_4}{l_4+s_3-s_4} & \cdots & 0 \\ & & \vdots & \vdots & & \\ & & 0 & 0 & & \end{bmatrix} \begin{bmatrix} \Delta s_0 \\ \vdots \\ \Delta s_3 \\ \Delta s_4 \\ \vdots \\ \Delta s_n \end{bmatrix} = \begin{bmatrix} \Delta\varepsilon_1 \\ \vdots \\ \Delta\varepsilon_4 \\ \vdots \\ \Delta\varepsilon_n \end{bmatrix}$$

The incremental strain in any rope segment may be related to the incremental tension by the use of a constitutive model for the rope. In this work a visco-elastic model is used with a spring in series with an in-parallel combination of another spring and dashpot (Fig. 6). In general, the quantities defining the rope model may be made a function of strain, but here these quantities have been set to constant values. Therefore, for rope segment i

$$\begin{aligned} \Delta T_i &= k_1\Delta\varepsilon_i + \frac{\Delta t}{\lambda}[k_1k_2\varepsilon_i - T_i(k_1+k_2)] \\ &= k_i\Delta\varepsilon_i + \Delta T_i^0 \end{aligned} \tag{11}$$

where k_1, k_2 and λ are the constants in the material model. Any model for the rope may be used,

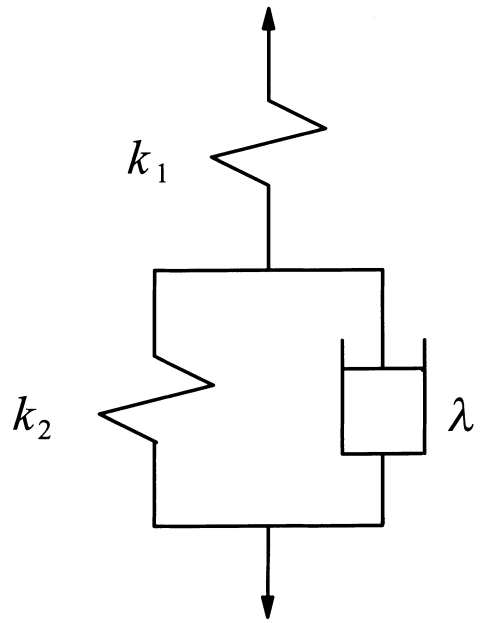

Figure 6 Visco-elastic model of a rope.

provided it can be written in a form relating increments of tension to increments of strain [as in eqn (11)].

A matrix equation is written giving the vector of incremental tensions $\Delta\mathbf{T}$ in terms of the vector of incremental strains

$$\mathbf{K}\Delta\boldsymbol{\varepsilon} = \Delta\mathbf{T} - \Delta\mathbf{T}^0 \tag{12}$$

where $\Delta\mathbf{T}^T = [\Delta T_1 \ldots \Delta T_i \ldots \Delta T_n]$ and $\Delta\mathbf{T}^{0T} = [\Delta T_1^0 \ldots \Delta T_i^0 \ldots \Delta T_n^0]$. Matrix $\mathbf{K}$ is of dimension n by n and is given by $\mathbf{K} = k_1\,\mathbf{I}$, where $\mathbf{I}$ is the n by n unit matrix.

At each runner slip may occur depending on the magnitude of the tension in the rope segments either side of the runner. If slip does occur the incremental tensions vary according to the tension ratio for the runner. These conditions for runner i are expressed as:

$$\begin{aligned}
&\Delta T_i = \eta_i \Delta T_{i+1};\ \Delta s_i < 0;\ \sigma_i = -1 \text{ if } T_i = \eta_i T_{i+1} \\
&\Delta s_i = 0;\ \sigma_i = 0; \quad \text{if } \eta_i T_{i+1} < T_i < \frac{T_{i+1}}{\eta_i} \\
&\Delta T_i = \frac{\Delta T_{i+1}}{\eta_i};\ \Delta s_i > 0;\ \sigma_i = +1 \quad \text{if } T_i = \frac{T_{i+1}}{\eta_i}
\end{aligned} \tag{13}$$

where σ_i is used to specify the slip condition.

It is assumed that slip occurs at the belay if the tension in the first rope segment is equal to a critical value. The condition for slip at the belay is expressed as:

$$\begin{aligned}
&\Delta s_0 = 0;\ \sigma_0 = 0 \quad \text{if } T_1 < S \\
&\Delta T_1 = 0;\ \Delta s_0 > 0;\ \sigma_0 = +1 \quad \text{if } T_1 = S
\end{aligned} \tag{14}$$

where S is the critical tension in the first rope segment.

Equations (13) and (14) can be used to derive a matrix equation relating the incremental tensions

$$\mathbf{L}\Delta\mathbf{T} = 0 \tag{15}$$

Each row of matrix $\mathbf{L}$ corresponds to a slip condition where σ_i is nonzero. For example, if the slip condition at runner 3, σ_3, is equal to $+1$, the corresponding row of matrix $\mathbf{L}$ has the form:

$$\begin{bmatrix} & & 0 & 0 & & \\ & & \vdots & \vdots & & \\ 0 & \ldots & 1 & -1/\eta_3 & \ldots & 0 \\ & & \vdots & \vdots & & \\ & & 0 & 0 & & \end{bmatrix} \begin{bmatrix} \Delta T_1 \\ \vdots \\ \Delta T_3 \\ \Delta T_4 \\ \vdots \\ \Delta T_n \end{bmatrix} = \begin{bmatrix} 0 \\ \vdots \\ 0 \\ \vdots \\ 0 \end{bmatrix}$$

It has been found necessary to use a modified form of eqn (15) to avoid instabilities when the size of increment is other than very small:

$$\mathbf{L}\Delta\mathbf{T} = -\mathbf{L}\mathbf{T} \tag{16}$$

where the vector of rope tensions $\mathbf{T}^T = [T_1 \ldots T_i \ldots T_n]$. Equations (15) and (16) are identical provided eqn (15) has been satisfied exactly for all previous increments.

Equations (10), (12) and (16) may now be combined to give a set of linear equations that can be solved to find the vector of incremental slips, $\Delta\mathbf{s}$.

$$\mathbf{LKC}\Delta\mathbf{s} = -\mathbf{L}[\mathbf{T} + \Delta\mathbf{T}^0] \tag{17}$$

At the end of each increment, the incremental strains are calculated from the incremental slips by eqn (10). The incremental tensions are then found

by eqn (12) and the current rope tensions incremented, taking account that the rope tensions must be always greater than or equal to zero. Finally the new velocity of the leader v can be found from

$$v = \dot{s}_n + (g - T_n/M)\Delta t.$$

A computer program has been written to carry out the calculations described above. The duration of the time increment Δt is set small enough to achieve good accuracy, but it is found that the numerical calculations are well-behaved and largely insensitive to the duration of the increment, provided it is small enough.

Comparison of theoretical and experimental simulations

The theoretical analysis of climbing falls presented above are now used to simulate climbing falls, providing predictions of the tension developed in the rope. These predictions are compared with measurements of tension taken from experimental simulations of climbing falls.

The experimental apparatus consisted of a trolley running on a vertical steel column as shown in Fig. 7. Extra lead bars could be added to alter the mass of the trolley up to a maximum of 80 kg. A catch at the top of the steel column held the trolley in the raised position until a test was carried out.

Two belay mounts equipped with strain gauges were used, one to represent a running belay bolted to the column, the other to represent the second's belay, bolted to the floor. The belay mounts were manufactured so as to have similar cross sections to standard karabiners. Strain gauges were attached to the belay mounts in a full-bridge configuration and connected to Fylde type FE-492-BBS bridge conditioners and FE-254-GA amplifiers. The output from the strain gauge amplifiers was recorded during a test using a Datalab DL1200 datalogger with a sampling interval of 500 μs. The tensions in

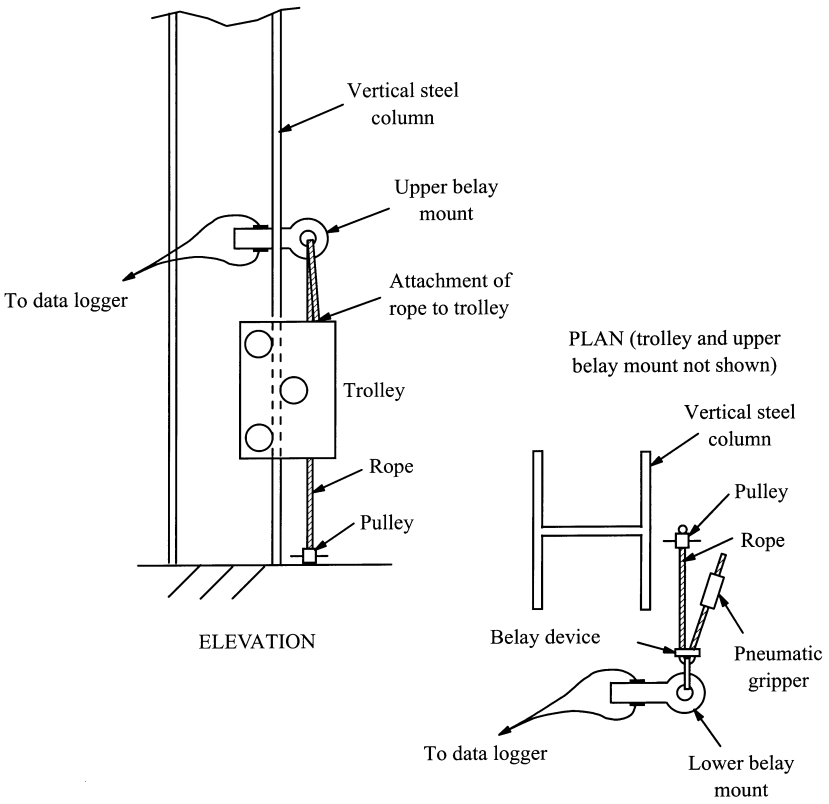

Figure 7 Details of experimental apparatus.

the two rope segments during the test were derived from the loads measured by the belay mounts.

The rope used was Edelweiss M/W V.31 of diameter 8.7 mm. The rope was tied to the trolley, fed through the running belay then back to the belay device. The grip of the second's hand on the rope wass simulated using a pneumatic gripper as shown in Fig. 7. The gripper allowed different tensions to be applied to the rope running through the belay device and different angles to be set for the rope either side of the belay device. The gripper was designed so as to be able to apply a higher load than a human second would find possible.

Before a theoretical simulation could be undertaken, the parameters used to model the mechanical behaviour of the climbing rope had to be derived by experiment. The behaviour of the rope could not be measured using a conventional tensile test machine since the rope can suffer large strains and exhibits a strong strain rate dependency. The method used here wass to load the rope dynamically using the falling trolley and record the tension in the rope as a function of time. No running belay was used and the rope was tied off at the belay so that the measurements related purely to the behaviour of the rope. The acceleration of the trolley could be calculated from the tension in the rope and hence the position of the trolley and therefore the strain in the rope could be derived by a process of double integration.

The tension vs. strain response for a typical test is shown in Fig. 8. This test used a 2.1-m length of rope, a fall factor of 1.3 and a trolley mass of 40 kg. One test provided the complete response since the rope was loaded to the maximum tension and then relaxed to zero as the trolley returned upwards. The rope behaved in a significantly nonlinear fashion and exhibited considerable hysterisis. The nonlinearity of the rope was most noticeable at low strains due to the fibres in the rope aligning themselves with the loading direction. The hysterisis was a result of the friction between adjacent fibres and the damping behaviour of the nylon fibres themselves. The experimental trace shows a superimposed oscillation which is believed to be a result of tension waves in the rope.

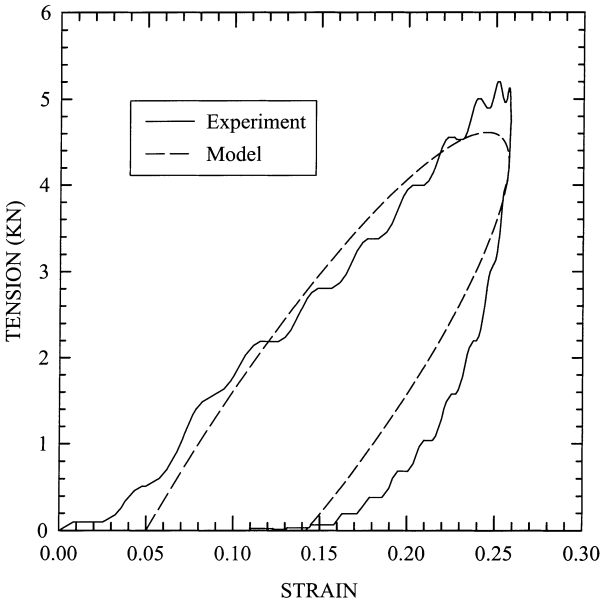

Figure 8 Tension vs. strain from a dynamic test on a rope compared with the model.

For the purposes of the theoretical analysis of climbing falls conducted here, it was felt to be sufficient to model the rope using the linear viscoelastic model shown in Fig. 6, but including an initial strain offset so that the rope only begins to take tension once a certain value of strain has been exceeded. This provides a straightforward method of including the significant nonlinearity of the rope at low strains. Values for the spring and dashpot parameters in the model were chosen to give an adequate match with the measured tension vs. strain curve in Fig. 8. No direct procedure exists to derive values directly for the various parameters, since the strain rate varies during the test. The values for the chosen parameters are:

$k_1 = 35.0$ kN
$k_2 = 20.0$ kN
$\lambda = 3.0$ kN s^{-1}
$\varepsilon_0 = 0.05$

where ε_0 is the initial strain offset. The strain offset can be included in the existing theoretical simulation, merely as a factor on the initial length of the rope.

The theoretical technique may now be used to provide predictions of tension vs. time that

can be compared with the experimental results. Figure 9(a,b) shows two such comparisons. The tension given refers to the segment of rope between the running belay and the trolley. The mass of trolley, length of rope and fall factor for these comparisons are given in Table 1.

A typical trace of tension for the case of the rope tied off at the belay is shown in Fig. 9(a). The tension rises quickly to a maximum of 2.6 kN, then decays more gradually to zero. Two smaller peaks then occur, after which the tension remains constant at a value corresponding to the weight of the trolley. The theoretical simulation agrees well with the experimental measurements, particularly for the maximum tension.

Figure 9(b) shows a typical trace with a Stitch plate, a common belay device. The tension rises quickly to a maximum of 1.9 kN, then drops slightly to a small plateau of 1.6 kN before falling to zero. There is then a small second peak after which the tension remains at a constant value equal to the weight of the trolley. The cause of the small initial peak is the behaviour of the pneumatic gripper where the tension to initiate slip through the gripper is higher than that for slip to continue. The theoretical simulation assumes a constant value for the critical tension for slip at the belay and is therefore unable to predict the small drop in load after the initial peak that occurs in the test results. The theory is thus unable to provide a wholly accurate simulation when slip through the belay occurs.

Prediction of rope failure

The theoretical simulation of climbing falls provides predictions of the tension in rope segments and the slip at running belays. A useful simulation would provide additional information concerning the damage to the rope that could be used to assess the lifetime of a rope. The precise mechanisms of rope damage are largely unknown, therefore a programme of experimental work has been undertaken using the same apparatus as has already been described.

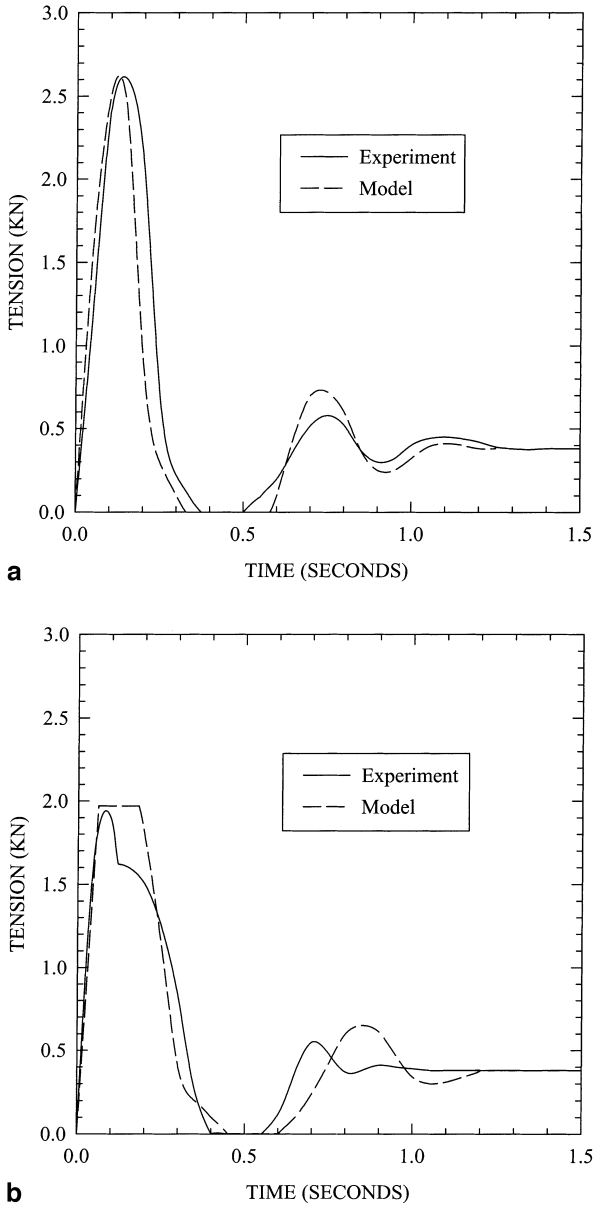

Figure 9 Comparison of experimental and theoretical simulations of the tension in the rope (a) for the case of a fall with the rope tied off at the belay and (b) for the case of a fall with a Stitch plate at the belay.

Table 1 Test details for comparisons between experimental and theoretical simulations

Figure	Belay condition	Length of rope (m)	Fall factor	Mass (kg)	Runner radius (mm)
9(a)	Tied off	4.0	0.50	40	6.0
9(b)	Stitch plate	4.9	0.54	40	6.0

Rope failure inevitably occurs where the rope runs through the running belay. Typically, several falls are required to cause rope failure depending on the fall factor, length of fall, mass of climber and whether a belay device was used or the rope tied off. A critical factor was identified as the edge radius of the belay mount used to represent the running belay. Belay mounts were manufactured with different radii varying from 2 mm to 6 mm. The smaller radius was designed to simulate the rope running over a sharp rock edge, whereas the larger radii were intended to match the cross section of standard karabiners.

It is proposed that the damage to the rope as it runs over the running belay depends on the rate of energy dissipation through frictional losses. The tension T_2 in the rope segment due to friction between the running belay and falling climber is greater than the tension T_1 in the segment between the running and fixed belays (Fig. 3). These tensions are related by the tension ratio η for the running belay so that $T_2 = \eta T_1$. The rate of energy dissipation $\dot{E}$ at the running belay therefore is given by

$$\dot{E} = \dot{s} T_2 \left[1 - \frac{1}{\eta}\right] \tag{18}$$

where $\dot{s}$ is the rate of slip. However, any one section of rope dissipates an amount of energy proportional to $T_2(1 - 1/\eta)$ since, although the rate of energy dissipation increases with $\dot{s}$, so too does the rate at which the rope runs through the belay. Therefore, it is proposed that the damage to the rope depends on the maximum value of tension generated during a fall. However, since the energy dissipation by any section of rope is increased by a smaller radius of runner this dependency on tension will be altered with a different radius of runner.

Table 2 provides results of the number of falls-to-failure and the maximum tension recorded in the rope between the running belay and the trolley. A measurement of four falls-to-failure, for example, means that the rope failed during the fourth fall. For severe falls, the rope mantle and kern of the rope fail together as seen in Fig. 10(a). For less severe falls, however, the mantle of the rope fails before the kern [Fig. 10(b)]. Following mantle failure, a number of extra falls are required to cause failure of the kern. The number of falls-to-failure in Table 2 relates to complete failure of the rope: kern and mantle. Various conditions for a fall were considered: different trolley mass, runner radius, fall factor and length of rope. Most of the tests were carried out with the rope tied off at the belay, but for two tests a Stitch plate was used in conjunction with the pneumatic gripper. The two test results for the Stitch plate were derived using different gripper pressures.

Table 2 Number of falls to failure for various fall conditions

Belay condition	Runner radius (mm)	Mass (kg)	Fall factor	Length of rope (m)	Falls to failure	Maximum tension (kN)
Tied off	6.0	60	0.86	2.50	15	5.7
Tied off	6.0	60	1.32	2.50	5	7.1
Tied off	6.0	60	1.77	2.50	4	8.2
Tied off	6.0	70	0.40	2.50	18	4.3
Tied off	6.0	70	0.80	2.50	10	5.9
Tied off	6.0	70	0.86	2.50	9	6.2
Tied off	6.0	70	0.87	1.50	4	6.1
Tied off	6.0	70	0.90	1.50	4	6.4
Tied off	6.0	70	0.90	1.50	9	6.2
Tied off	6.0	70	0.90	1.50	7	6.3
Tied off	6.0	70	0.97	2.50	8	6.5
Tied off	6.0	70	1.00	1.00	11	6.5
Tied off	6.0	70	1.00	1.33	9	6.6
Tied off	6.0	70	1.00	2.00	9	6.8
Tied off	6.0	70	1.32	2.50	5	7.6
Tied off	6.0	70	1.77	2.50	3	8.8
Tied off	6.0	80	0.86	2.50	7	6.6
Tied off	6.0	80	0.97	2.50	8	7.0
Tied off	6.0	80	1.32	2.50	4	8.2
Tied off	6.0	80	1.77	2.50	3	9.4
Tied off	4.0	70	0.40	2.50	11	4.2
Tied off	4.0	70	0.40	2.50	10	4.3
Tied off	4.0	70	0.90	1.50	7	6.3
Tied off	4.0	70	0.90	1.50	3	6.2
Tied off	4.0	70	1.33	2.00	4	7.7
Tied off	2.0	70	0.40	2.50	5	4.3
Tied off	2.0	70	1.33	2.00	2	7.8
Stitch plate	6.0	70	0.22	4.50	43	2.6
Stitch plate	6.0	70	0.22	4.50	27	4.0

The test results support the implications of the simple analytical model that the maximum tension, and hence the number of falls-to-failure, principally depend on the fall factor, mass of climber and runner radius. It is particularly noticeable how the use of a belay device reduces the maximum tension and greatly increases the number of falls to failure.

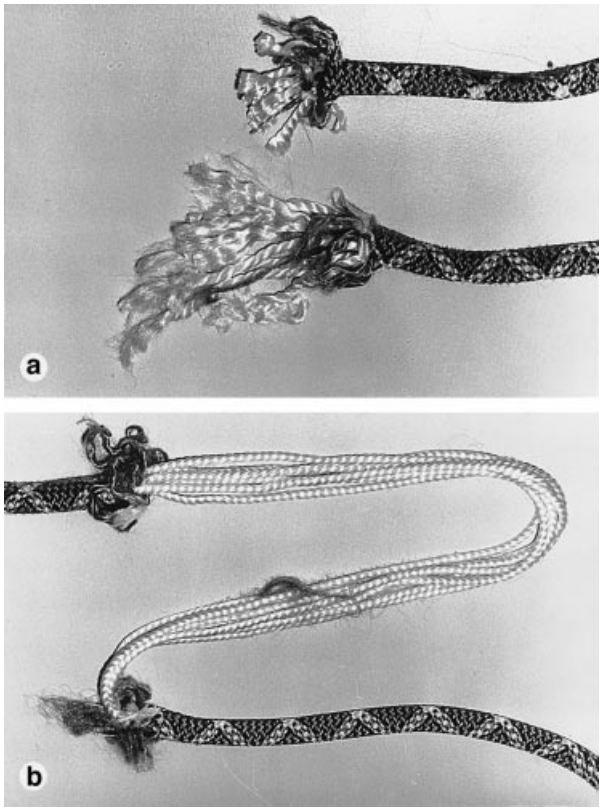

Figure 10 Ropes showing (a) kern failure and (b) mantle failure.

Figure 11 shows the data of Table 2 plotted as the maximum tension vs. the number of falls to failure for the three different runner radii considered in the tests. Error bars of plus or minus one fall are included since it is not known how close to failure the rope is after each fall. The data is plotted in a similar manner to a conventional stress amplitude vs. cycles to failure fatigue curve. It can be appreciated that reducing the radius of the runner for the same maximum tension generated in the fall substantially reduces the number of falls-to-failure.

If the proposed mechanism of rope failure is valid, the data for one radius of runner should be shrunk onto one curve. The data is reasonably consistent with this proposed mechanism; a line is superimposed on the graph showing a linear fit to the data for a runner radius of 6 mm. Fall conditions below this line can be thought of as safe, while for those above this line, rope failure is likely to occur.

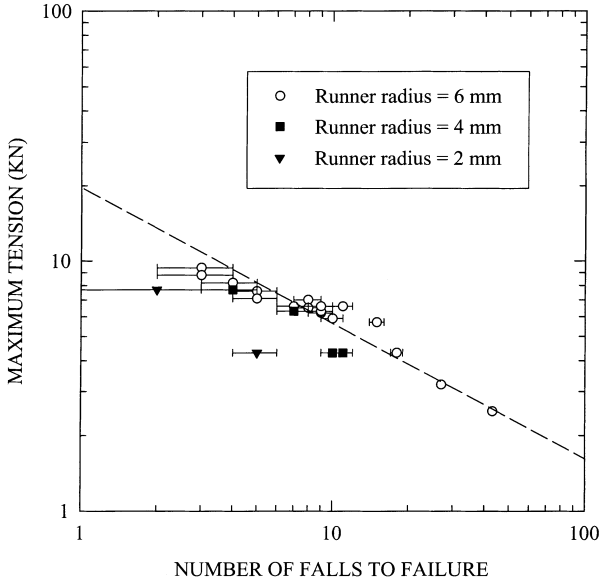

Figure 11 Maximum tension vs. the number of falls to failure.

Discussion

The theoretical simulation of climbing falls that has been developed in this paper includes the major phenomena influencing the tension developed in a climbing rope. In the case of the rope tied off at the belay, the theoretical predictions match closely the observed experimental behaviour. Predictions are less good when slip at the belay occurs, largely because a simple model has been used for the behaviour of the belay device. Certainly a more sophisticated model could be used, for example by including a critical tension to initiate slip at the belay followed by a lower value for slip to continue.

The visco-elastic model used for the rope is characterized by three constant parameters, with a strain offset to allow some account to be taken of nonlinearity at low strains. The derivation of the parameters of the rope model is currently achieved using an *ad hoc* approach. A more systematic method is required to derive a rope behaviour model, but this is likely to require special purpose test equipment to allow dynamics tests to be carried out under constant strain rate conditions.

Since the mass of the rope itself was not included in the analysis, the model is unable to predict the

size of tension waves in the rope. For a linear elastic rope the magnitude of these tension waves can be predicted from Timoshenko & Goodier (1982):

$$T = vcm \tag{19}$$

where T is the magnitude of the wave, v is the velocity of the climber just before the rope becomes tight, c is the velocity of propagation of waves in the rope given by $c = \sqrt{k/m}$ and m is the mass per unit length of the rope. Using typical values, the magnitude of the tension waves may be found to be much less than the predicted tensions neglecting the mass of the rope. Conversely, tension waves in polymer ropes used for mooring ships are significant, but the behaviour of these ropes is very different from a climbing rope (Leeuwen 1981).

It has been proposed that the failure of a rope is related to the dissipation of friction as the rope runs over the running belay. Certainly, evidence exists that melting and abrasion of the mantle does occur. Experimental data of the maximum tension vs. the number of falls-to-failure does support this proposed failure mechanism and enables a safe working envelope to be constructed to ensure rope failure does not occur. However, no account is taken of environmental factors such as grit working its way into the kern. Tests have been carried out to examine such effects, demonstrating considerable differences between new and environmentally damaged ropes in the number of falls to failure (Pavier 1998).

The severity of damage to the rope has been assessed by the number of falls to failure. Although this approach appears to work for the case of a number of identical falls it is difficult to extend it to the more general situation where one rope experiences a number of different falls. Not only do different falls create different magnitudes of tension, but also different falls do not damage the same section of the rope. Although in principle the effect of different falls could be taken into account, it is unlikely that a climber would record the history of the rope in sufficient detail to allow an accurate assessment of remaining life to be made. The work that has been described in this paper is likely to be of most practical use in giving a better qualitative understanding of the factors that determine the lifetime of a rope.

Conclusions

A theoretical simulation of climbing falls has been developed, allowing good predictions to be made of the tension generated in the rope. The simulation includes slip of the rope through the belay device, friction at runners and a visco-elastic model for the rope. The simulation can be extended to account for more general nonlinearity of the rope behaviour and a more sophisticated simulation of the belay device.

Experimental testing has provided information on the number of falls-to-failure for different fall situations. The data show that the number of falls can be related to the tension developed at the running belay. The theoretical simulation may therefore be used to enable predictions to be made of the number of falls-to-failure for a general fall situation.

References

Leeuwen, J.H.V. (1981) Dynamic behaviour of synthetic ropes, *Proc 13th Offshore Technology*, 453–463, Texas.

Microys, H.F. (1983) *Summit*, 31,.

Pavier, M.J. (1996) Derivation of a rope behaviour model for the analysis of forces developed during a rock climbing leader fall. *Proceedings of the 1st International Conference on the Engineering of Sport* (ed. S.J. Haake), 271–279, A.A. Balkema, Rotterdam.

Pavier, M.J. (1998) Failure of climbing ropes resulting from multiple leader falls. *Proceedings of the 2nd International Conference on the Engineering of Sport* (ed. S.J. Haake), 415–422, Blackwell Science, Oxford.

Perkins, A. (1987) *Development of Fall Arrest Equipment Using Textiles*, PhD Thesis, University of Leeds.

Schubert, P. (1986). *Ausrustung, Sicherung, Sicherheit*. BLV-Verlagsgesellschaft, Munich.

Smith, R.A. (1996) The development of protection systems for rock climbing. *Proceedings of the 1st International Conference on the Engineering of Sport* (ed. S. Haake), 229–238, A.A. Balkema, Rotterdam.

Timoshenko, S.P. & Goodier, J.N. (1982) *Theory of Elasticity*, 3rd edn. McGraw-Hill, New York.

Wexler, A. (1950) The Theory of Belaying, *American Alpine Journal*, **7**, 379–405.